

RSC Advances



This is an *Accepted Manuscript*, which has been through the Royal Society of Chemistry peer review process and has been accepted for publication.

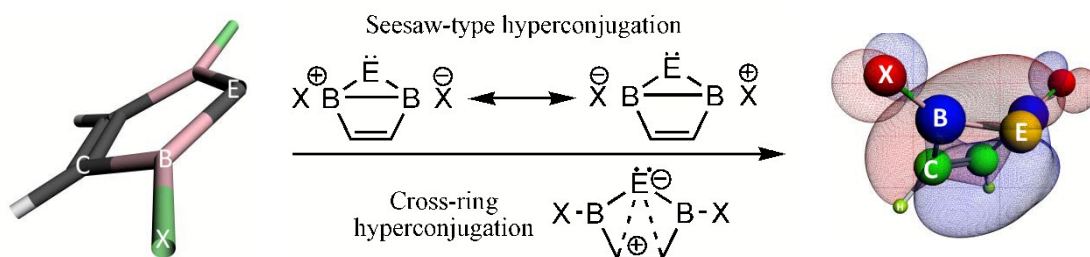
Accepted Manuscripts are published online shortly after acceptance, before technical editing, formatting and proof reading. Using this free service, authors can make their results available to the community, in citable form, before we publish the edited article. This *Accepted Manuscript* will be replaced by the edited, formatted and paginated article as soon as this is available.

You can find more information about *Accepted Manuscripts* in the [Information for Authors](#).

Please note that technical editing may introduce minor changes to the text and/or graphics, which may alter content. The journal's standard [Terms & Conditions](#) and the [Ethical guidelines](#) still apply. In no event shall the Royal Society of Chemistry be held responsible for any errors or omissions in this *Accepted Manuscript* or any consequences arising from the use of any information it contains.

Graphical and text abstract

Interesting π - and σ -bond hyperconjugations cause the unusual stability of the puckered Arduengo type divalents with electron deficient boron atoms.



Cite this: DOI: 10.1039/c0xx00000x

www.rsc.org/xxxxxx

ARTICLE TYPE

A quest for stable 2,5-bis(halobora)cyclopentenylidene and its Si, Ge, Sn and Pb analogs at theoretical levels

Alireza Akbari,^a Babak Golzadeh,^a Sattar Arshadi^a and Mohammad Zaman Kassae^b

Received (in XXX, XXX) XthXXXXXXXXXX 20XX, Accepted Xth XXXXXXXXXXXX 20XX

DOI: 10.1039/b000000x

Replacing the two nitrogen atoms of Arduengo's N-heterocyclic carbenes (NHCs) with electron deficient boron atoms forms B-heterocyclic carbenes (BHCs) which may appear destabilizing at the first glance. Yet, among 40 optimized singlet (s) and triplet (t) BHCs and their Si, Ge, Sn and Pb homologues (BHĒs), eight species are found that show higher stability than their corresponding NHĒs for exhibiting wider singlet-triplet energy gaps (ΔE_{st}), at B3LYP/TZ2P, as well as CBS-QB3 and G4MP2 *ab initio* levels. Moreover, triplet BHĒs assume planar geometry with the dihedral angle (D1) of about zero degrees. In contrast, their corresponding singlets show a high tendency for puckering with $D1 \cong 66^\circ$. The preference of the latter for puckered nonplanar geometries is evidenced by NBO calculations and visually through their frontier molecular orbitals. Main stabilizing interactions appear to be π - and σ -bond hyperconjugation across the ring. The resulting eight species that demonstrate higher stability are: 2,5-bis(iodobora)cyclopentensilylene, 2,5-bis(Z-bora)cyclopenten-germylene and -stannylene, for Z=Br and I; as well as 2,5-bis(Z₂-bora)cyclopentenplumbylene, for Z₂=Cl, Br and I.

1. Introduction

Now as ever before, researchers are fascinated with group 14 divalents including carbenes,¹⁻⁵ silylenes,⁴⁻⁶ germlylenes,^{2, 4, 5, 7, 8} stannylenes,^{4, 5, 7, 9, 10} and plumbylenes.^{5, 10, 11}

-As for carbenes, immense interest was regenerated upon the isolation and characterization of the first stable one, called N-heterocyclic carbene (NHC), by Arduengo in 1991.¹²⁻¹⁵ This appeared in a clear contrast to "the parent" highly reactive methylene (:CH₂), once labelled as "the most indiscriminate reagent in organic chemistry".¹⁶ Nevertheless, most acyclic and/or alkyl carbenes tend to be intrinsically triplet with rather high reactivity.

The scenario totally changes on going from carbene to its homologues metallylenes (silylene, germylene, stannylene and plumbylene). In so doing, multiplicity may alter from triplet to singlet, while the stability increases (on descending group 14). This phenomenon is attributed to the "inert pair effect", where s electrons become progressively lower in energy upon descending the group.¹⁷

-Arduengo type N-heterocyclic silylenes (NHSis) constitute the vast majority of such species with different stability and diverse structure and reactivity. Among them is that reported by Denk *et al.* in 1994.¹⁶ These practically started after the seminal work of Atwell and Wyenberg on the matrix isolation of transient Me₂Si: in 1960s.¹⁸

-As for germlylenes, they have been the center of attention due to their importance in chemical vapour deposition, semiconductor manufacturing, photonics, and aerospace industries.¹⁹⁻²¹ Long before their carbene homologues, N-heterocyclic germlylenes

were developed by Veith and Meller.^{22, 23}

-Considerable progress has been made in the chemistry of stable derivatives of divalent tin.^{24, 25} Specifically, N-heterocyclic stannylenes (NHSns) have received their share of great attention.²⁶⁻²⁹

-Finally, dialkyl and diarylplumbylenes have been isolated and characterized by Lappert *et al.*³⁰⁻³² Despite the toxicity of lead which has somewhat hampered its scrutiny, several examples of N-heterocyclic plumbylenes (NHPbs) have surfaced.^{23, 33, 34}

Moreover, there are some carbenes which contain one or more boron atoms in their cyclic structures,³⁵ or appear as the boryl anion.³⁶⁻⁴¹ Synthesis of phosphino(boryl)methanes⁴² is recently been followed by theoretical investigations on the reactivity of acyclic boryl(phosphino)-based B-Ē-P species which suggests that the relative divalent reactivity decreases in the order C > Si > Ge > Sn > Pb.⁴³ In other words, the heavier is a group 14 atom (E), the more is its stability.

Unstable four-membered species containing B-Ĉ-B carbene moieties were characterised long ago.^{44, 45} Recently, by making use of the strong σ -donor properties and high steric loadings, monomeric species, Sn{B(NDippCH)₂}{N-(SiMe₃)Dipp} and Sn{B(NDippCH)₂}₂ were synthesized in solid state.⁴⁶

Here, we have set up to study boron-heterocyclic carbenes (BHCs) where the nitrogen atoms of an Arduengo cyclic carbene are replaced with electron deficient boron atoms. In fact, the substitution of nitrogens with borons in NHCs means a change from p⁶ electron-rich system (of the two nitrogens) to a p² electron deficient system (of the two borons). In particular, following up on our quest for more stable halogenated group 14 divalent species,⁴⁷⁻⁵¹ in this manuscript we have carried out

comparative theoretical studies on possible configurations of singlet and triplet⁵² of $C_2H_2B_2EX_2$ ($\ddot{E} = C$; $X = F, Cl, Br$ and I) as well as their group 14 divalent homologues ($\ddot{E} = Si, Ge, Sn,$ and Pb). In addition, to give a more clear physical picture about the thermodynamic stabilities of $BH\ddot{E}s$, some isodesmic reactions are employed which show the tendency of carbene dimerization, hydrogenation, coupling, as well as carbenoid formation with Cu, Ag and Au .

2. Computational details

Divalent species and their corresponding metal complexes (Figs. 1 and 2, respectively) are optimized at UB3LYP⁵³, and second-order Møller–Plesset perturbation, UMP2, using 6-311++G** basis set⁵⁴ of the GAUSSIAN 98⁵⁵ and an analogous basis set (TZ2P; Triple zeta double polarized) in the ADF system of programs.⁵⁶⁻⁵⁸ Moreover, optimizations are carried out on all $BH\ddot{E}s$, other than those containing heavy atoms ($1_X, 2_X, 3_X, 4_X$ and 5_X), using the high accuracy CBS-QB3 and G4MP2 methods.

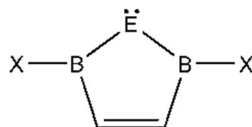


Fig. 1 A general structure for 40 structures optimized in this work including: Carbenes ($\ddot{E} = C$: $1_{s-X}, 1_{t-X}$); Silylenes ($\ddot{E} = Si$: $2_{s-X}, 2_{t-X}$), Germlynes ($\ddot{E} = Ge$: $3_{s-X}, 3_{t-X}$), Stannylenes ($\ddot{E} = Sn$: $4_{s-X}, 4_{t-X}$), and Plumbylenes ($\ddot{E} = Pb$: $5_{s-X}, 5_{t-X}$)

Global minima are specified on the corresponding energy surfaces through relax scan using keyword “FOPT (Z-matrix)” at UB3LYP/6-311++G** level of theory. Obtained minimum via scanning, the latter are used as inputs for the UB3LYP/6-311++G** (basis set of McGrath,⁵⁹ Curtiss⁶⁰ included the diffuse functions) calculations. This is for obtaining more accurate values of optimized geometries, energetic parameters, orbital interactions and electronic configurations. Single-point calculations on the “second order perturbation theory analysis of fock matrix in natural bonding orbitals (NBO) basis” which summarizes the second order perturbative estimates of donor-acceptor (bond-antibond) interactions in the NBO basis are also performed.

All divalent species with heavy or transition atoms ($I, Sn, Pb, Cu, Ag,$ and Au) acquire spin-orbit interactions, calculated using “Extrabasis” keyword (LANL2DZ, McGrath-Curtiss basis set, in the GAUSSIAN 98⁶¹), and zeroth order relativistic approach (ZORA⁶²⁻⁶⁶, in the ADF program). To confirm the nature of the stationary species, frequency calculations are carried out. For minimum state structures, only real and positive frequency values are accepted.

3. Results and Discussion

We begin discussing our calculated data on novel $BH\ddot{E}s$ (Fig. 1), by estimating their stability through singlet-triplet energy gaps (ΔE_{st}) and energetic advantages of puckering for singlet states. Then we take up the effects of geometrical parameters and orbital interactions on the stability of the divalents. The discussion is continued by characterization of the scrutinized species through

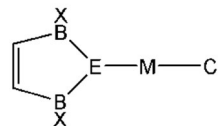


Fig. 2 Schematic representation for $1_X, 2_X,$ and 3_X-MCl ($X = F, Cl, M = Cu, Ag, Au$)

their electronic configurations, electrophilicity, nucleophilicity, isodesmic reactions and the study of their metal complexes (Fig. 2).

3.1 Singlet-triplet energy gap (ΔE_{st})

Singlet states of all $BH\ddot{E}s$ appear puckered with more stability than their corresponding planar triplets for showing relatively higher values of ΔE_{st} (Tables 1, 1S, 2S, 3S, 4S, Fig. 1 and 1S [Supplementary]).

Table 1 Comparison between singlet-triplet energy gaps, ΔE_{st} , (in kcal/mol) of carbenes (1_X) with heavier group 14 divalents including silylenes (2_X), germlynes (3_X), stannylenes (4_X) and plumbylenes (5_X), with $X = F, Cl, Br$ and I , at UB3LYP/TZ2P.

X	1_X	2_X	3_X	4_X	5_X
F	0.51	22.78	23.86	21.99	27.40
Cl	4.29	27.18	28.12	26.79	34.79
Br	4.85	27.80	28.70	27.47	33.96
I	5.58	29.14	30.06	28.85	39.98

On the basis of ΔE_{st} , carbenes (1_X) emerge considerably less stable than their corresponding silylenes (2_X), germlynes (3_X), stannylenes (4_X) and plumbylenes (5_X). In other words, the stability order of our sextet divalent species generally increases on descending group 14 (to be discussed in more details in sections 3.3 and 3.4.2). This conveys a small drop from 3_X to 4_X in UB3LYP/TZ2P level which is not encountered when MP2, G4MP2 and CBS-QB3 are employed (Supplementary Tables 2S-4S, respectively).

As to ΔE_{st} of 1_X-3_X ($X = F, Cl, Br$), the performance of the B3LYP functional relative to those at the CBS-QB3 and G4MP2 levels is determined^{67, 68} (Table 2). This assessment is demonstrated *via* absolute (column (a) and (b) in Table 2) and mean absolute errors (MAE). As the latter indicates, deviation of B3LYP with G4MP2 level is smaller than that with CBS-QB3.

Table 2 Absolute and mean absolute errors on ΔE_{st} calculated with B3LYP functional relative to CBS-QB3 and G4MP2.

species	(a) CBS-QB3 $\Delta E_{B3LYP} - \Delta E_{CBS-QB3}$	(b) G4MP2 $\Delta E_{B3LYP} - \Delta E_{G4MP2}$
1_F	-0.91	-2.01
1_{Cl}	-0.03	-0.73
1_{Br}	-0.08	-0.86
2_F	3.97	2.79
2_{Cl}	5.57	4.69
2_{Br}	5.59	4.55
3_F	2.18	1.74
3_{Cl}	3.39	3.03
3_{Br}	3.32	2.77
Mean absolute errors	2.56	1.77

In addition to the above comparison between the stability of our boron substituted $BH\ddot{E}s$, it is interesting to compare and contrast the stability of our divalent species with their corresponding Arduengo's. At the first glance, such replacement of the two nitrogen atoms of Arduengo's N-heterocyclic carbenes, NHCs, with electron deficient boron atoms, BHCs, appears highly

destabilizing. Yet, among 40 optimized singlet and triplet BHĖs and their Si, Ge, Sn and Pb homologues (BHĖs), eight (**2**_I, **3**_{Br}, **3**_I, **4**_{Br}, **4**_I, **5**_{Cl}, **5**_{Br}, and **5**_I) are found which show higher stability than their corresponding NHĖs for exhibiting wider singlet-triplet energy gaps (ΔE_{st}) and hence a greater $\delta(\Delta E_{st}) = (\Delta E_{st}^{NHĖs} - \Delta E_{st}^{BHĖs})$ at UB3LYP/TZ2P (Table 3). Besides, **2**_{Br}, **4**_{Cl}, and **5**_F emerge energetically comparable with their NHĖ analogues. This is somewhat similar to the results obtained with other methods such as G4MP2 (Table 5S). In fact, calculations show a decrease of ΔE_{st} for NHĖs from lighter to heavier atoms of Ė and/or X. This means that from X=F to X=I and also descending group 14, the NHĖ species exhibits narrower singlet-triplet energy gaps (ΔE_{st}) which is in reverse to the analogues BHĖs. The G4MP2 results show larger ΔE_{st} for **2**_{Br}, **3**_{Cl} in addition to B3LYP results. Expanding the G4MP2 results demonstrates that they may acceptably cover B3LYP results, hence comparable ΔE_{st} between BHĖs and their NHĖ counterparts are obtained.

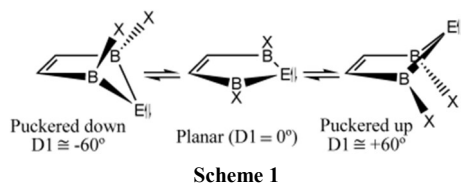
Table 3 Comparison between the stability of our divalent species (BHĖs: **1**_X-**5**_X) with their corresponding Arduengo's (NHĖs) by considering their energy differences, $\delta(\Delta E_{st}) = (\Delta E_{st}^{NHĖs} - \Delta E_{st}^{BHĖs})$, (in kcal/mol) at UB3LYP/TZ2P^a.

X	1 _X	2 _X	3 _X	4 _X	5 _X
F	58.24	34.08	19.97	10.34	2.03
Cl	35.68	12.56	8.02	4.30	-6.72
Br	23.11	2.67	-2.03	-4.25	-11.44
I	15.77	-1.37	-6.22	-11.49	-20.30

^aA negative sign indicates higher stability of BHĖs while positive numbers signify higher relative stability of NHĖs.

3.2 Puckering energy (PE)

Singlet state structures demonstrate energetic advantages through "puckering" (Scheme 1).



A clear contrast between energies of singlet and triplet BHĖs as a function of their divalent dihedral angle $D1(\angle C-B-\ddot{E}-B)$ is observed at UB3LYP/TZ2P (Fig. 3). For example an energy difference of 18 kcal/mol is encountered between the planar and fully puckered ($D1 \cong 60^\circ$) singlet chlorinated germylene **3**_{s-Cl} which decreases to 12 kcal/mol for the corresponding carbene **1**_{s-Cl} (Fig. 3, left). This is in contrast to the corresponding triplet state structures which prefer planarity and display an aversion to puckering (Fig. 3, right). Also an energy difference of 12.6 kcal/mol is encountered in favour of the planar structure vs. the puckered ($D1 \cong 45^\circ$) of triplet chlorinated germylene **3**_{t-Cl}. The same results are found when PE surfaces are sketched for the selected germylenes **3**_{s-X} v.s. **3**_{t-X} as a function of $D1$ (Fig. 1S). It seems that the empty valence shell p orbital of Ė has no tendency to overlap with the empty p orbitals of the boron atoms. This is anticipated, because of the instability of vinylic cation that may be the result of such an overlap. This argument is to be continued and established with more details in proceeding section.

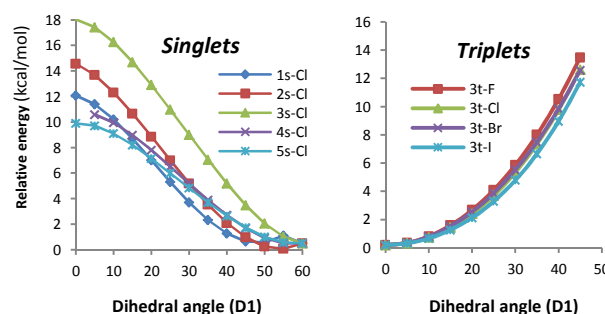


Fig. 3 Conspicuous contrast between energies of bis(boryl)-based divalents as a function of their dihedral angle $D1(\angle C-B-\ddot{E}-B)$ for puckered singlets (left, with the minimum at $\sim 60^\circ$) and planar triplets (right, with the minimum at 0°), at UB3LYP/TZ2P.

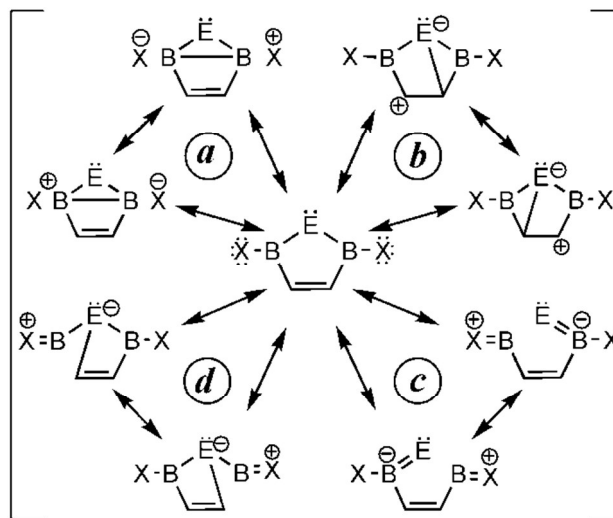
3.3 Geometric parameters and orbital interactions

Even though there is no experimental geometrical data for **1-5**, but a comparison of the theoretical structures with experimental geometries of related noncyclic B-Ė-B and B-Ė-N systems⁴⁴⁻⁴⁶ indicates that the calculated values may be accurate and reliable. The theoretically predicted Ė-B distances for Ė=C, Si, Ge and Sn with averages of 1.503, 2.039, 2.124 and 2.334 Å are in good agreement with the experimental values 1.515, 2.036, 2.141 and 2.334 Å, respectively.

Geometrical parameters of carbenes appear to be somewhat different and often in contrast to those of the rest of the group 14 divalents (Table 4, 6S).

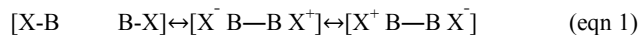
Divalent angle ($A1$) appears indirectly proportional to the Ė atomic size. So the largest $A1$ is found for carbenes while the smallest is that of plumbylens (Tables 3 and 6S, Fig. 2S).

An interesting interaction is hyperconjugation which we believe is the pretext for the puckerings of BHĖs discussed earlier in this study (Scheme 1). As a matter of fact, most geometrical parameters including bond lengths, bond angle, dihedral angle etc. appear consistent with our suggested hyperconjugation types of resonance (Scheme 2, Table 4, 6S).



For instance, there are evidences for an unprecedented seesaw-type hyperconjugation interaction for singlet species and not their

corresponding triplets (Scheme 2a). In order to focus on the B—B interaction we have simplified scheme 2a and written in the form of eqn 1:

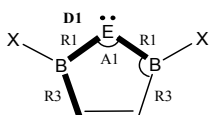


Interestingly, B—B distance appears shorter for every singlet state divalent compared to its corresponding triplet state (Table 4). For instance, B—B bond length for singlet species 1_{s-I} – 5_{s-I} are 2.29, 2.31, 2.36, 2.45 and 2.48 which are clearly shorter than those for their corresponding triplet states: 2.50, 2.88, 2.94, 3.05 and 3.26. This is consistent with significant Wiberg Bond Indices (WBI) for B—B interaction which decreases from iodine to fluorine in singlet BHĒs (eqn 1, Table 5).

Generally, the more polarizable a halogen (X), the more significant is the above hyperconjugation interaction (eqn 1).

Accordingly, divalents with iodine show the highest differences between their singlet-triplet B—B distances. Hence, the following general trend for the significance of eqn 1 is observed: $1_{s-I} - 5_{s-I} > 1_{s-Br} - 5_{s-Br} > 1_{s-Cl} - 5_{s-Cl} > 1_{s-F} - 5_{s-F}$.

Table 4 Selected bond length (R1 and R3) in Å, bond angle (A1) and dihedral angle (D1) in degrees, for the singlet BHĒs (1_X-5_X with X = F, Cl, Br and I) at UB3LYP/TZ2P.



Species	R1	R3	R4	B—B	A1	*D1
1_{s-F}	1.512	1.578	1.391	2.363(2.510)	102.8	58.3
1_{s-Cl}	1.503	1.577	1.390	2.343(2.521)	102.4	61.0
1_{s-Br}	1.500	1.575	1.391	2.348(2.513)	102.5	60.2
1_{s-I}	1.495	1.571	1.390	2.286(2.500)	99.7	61.4
2_{s-F}	2.051	1.545	1.399	2.449(2.868)	73.3	66.8
2_{s-Cl}	2.041	1.533	1.406	2.395(2.899)	71.9	72.1
2_{s-Br}	2.037	1.530	1.407	2.387(2.876)	71.1	71.1
2_{s-I}	2.027	1.526	1.409	2.313(2.882)	69.6	71.3
3_{s-F}	2.135	1.541	1.400	2.489(2.918)	71.3	66.8
3_{s-Cl}	2.128	1.529	1.407	2.451(2.952)	70.3	71.5
3_{s-Br}	2.122	1.526	1.406	2.451(2.948)	70.5	71.1
3_{s-I}	2.112	1.523	1.410	2.363(2.934)	68.0	71.2
4_{s-F}	2.356	1.543	1.395	2.624(3.041)	67.7	61.0
4_{s-Cl}	2.345	1.527	1.406	2.565(3.077)	66.3	68.0
4_{s-Br}	2.343	1.524	1.409	2.581(3.079)	66.8	67.8
4_{s-I}	2.332	1.518	1.412	2.452(3.049)	63.3	68.9
5_{s-F}	2.491	1.542	1.393	2.643(3.101)	64.1	59.8
5_{s-Cl}	2.477	1.527	1.402	2.586(3.283)	62.9	66.2
5_{s-Br}	2.473	1.525	1.404	2.585(3.279)	63.0	64.9
5_{s-I}	2.461	1.518	1.408	2.482(3.260)	60.6	65.8

Generally, the more polarizable a halogen (X), the more significant is the above hyperconjugation interaction (eqn 1). Accordingly, divalents with iodine show the highest differences between their singlet-triplet B—B distances. Hence, the following general trend for the significance of eqn 1 is observed: $1_{s-I} - 5_{s-I} > 1_{s-Br} - 5_{s-Br} > 1_{s-Cl} - 5_{s-Cl} > 1_{s-F} - 5_{s-F}$.

Now, let's summarize scheme 2b in eqn 2 where author pretext for puckering is illustrated through hyperconjugation.



For singlet divalents $1_X - 5_X$, rather significant $\ddot{E}-||$ are found

(Table 5).

Cross-ring hyperconjugation in our bis(boryl)-based heterocyclic divalents appear to be facilitated by the donor-acceptor interaction energies (Scheme 2b).^{69, 70}

Here the $BD(C=C) \rightarrow LP^*(\ddot{E})$ overlap (i.e. commonly written as $\pi \rightarrow p(\ddot{E})$) decreases from 1_{s-X} through 3_{s-X} which is consistent with the calculated WBI values. Fig. 4 demonstrates cross-ring hyperconjugation in 1_{s-F} , 2_{s-F} , and 3_{s-F} .

Schemes 2c and 2d are inspired from $\sigma \rightarrow p(B)$ and $\sigma \rightarrow p(\ddot{E})$ overlaps respectively (Table 5, 7S and 8S). The latter, in fact, is only significant in carbenes and decreases notably in its heavier homologues.

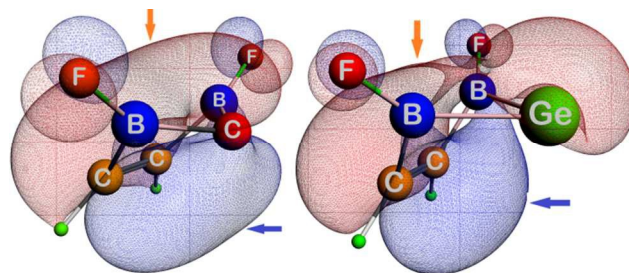


Fig. 4 Schematic depiction of the $\sigma \rightarrow p$ [B—B in scheme 2a] and $\pi \rightarrow p(\ddot{E})$ [scheme 2b] cross-ring hyperconjugative interactions as possible pretexts for puckering in 1_{s-F} and 3_{s-F} . The orange and blue arrows show the orbitals incorporated in these overlaps.

Table 5 Calculated “Wiberg bond indices” (WBI) for the singlet BHĒs (1_{s-X} , 2_{s-X} , 3_{s-X} , 4_{s-X} and 5_{s-X} with X = H, F, Cl, Br and I) at B3LYP/TZ2P and donor-acceptor energies (in kcal/mol) for most important interactions at B3LYP/6-311++g**.

Species	WBI		Donor-acceptor energies ^a		
	B—B	$\ddot{E}- ^b$	$\pi_{(C=C)} \rightarrow p(\ddot{E})$	$\sigma_{(B-E)} \rightarrow p(B)$	$\sigma_{(B-C)} \rightarrow p(\ddot{E})$
1_F	0.105	0.498	23.00	94.41	18.27
1_{Cl}	0.114	0.496	23.08	100.25	17.64
1_{Br}	0.113	0.494	21.87	101.81	17.1
1_I	0.123	0.472	---	---	---
2_F	0.235	0.394	13.62	15.63	4.68
2_{Cl}	0.278	0.400	15.27	17.58	4.36
2_{Br}	0.285	0.390	14.11	18.27	3.99
2_I	0.322	0.376	---	---	---
3_F	0.225	0.308	10.90	13.95	3.41
3_{Cl}	0.269	0.298	11.74	15.70	3.02
3_{Br}	0.279	0.294	11.65	16.26	2.78
3_I	0.323	0.284	---	---	---
4_F	0.214	0.246	^a the conventional statement for donor and acceptor orbitals		
4_{Cl}	0.269	0.254	^b is a symbol for C=C bond. The values of the $\ddot{E}- $ column are the products of the first column multiplied by 2		
4_{Br}	0.279	0.250	$(WBI_{(\ddot{E}-)} = WBI_{(\ddot{E}-CDB}) \times 2)$		
4_I	0.343	0.250			
5_F	---	---			
5_{Cl}	0.281	0.182			
5_{Br}	0.294	0.178			
5_I	0.362	0.180			

3.4 Electronic configurations

3.4.1 Frontier orbitals (FOs): In all carbenes, as well as 2_F , 2_{Cl} , 3_F and 4_F , the nonbonding σ (conventionally acknowledged as sp^2) orbital is the highest occupied molecular orbital (HOMO) and in 2_{Br} , 2_I , 3_{Cl} , 3_{Br} , 3_I , 4_{Cl} , 4_{Br} , 4_I , and all plumblylenes, this σ orbital is HOMO-1.⁷¹ The energy of this orbital with σ -symmetry increases with increasing the divalent atomic radius. Table 9S, represents the percentage for the contribution of the most populated atomic orbitals in the HOMO (and HOMO-1 anywhere

needed) and lowest unoccupied molecular orbital (LUMO) of divalent atom in all BH \ddot{E} s. The energy of each orbital is included in Table 9S.

Furthermore, the gap between HOMO and LUMO ($\Delta E_{\text{LUMO-HOMO}}$) decreases from silylenes to plumblylenes. Schematic view of FOs for $\mathbf{3}_{\text{s-Br}}$ (employed as an example) along with the relative MO level energies of a series of bis(boryl)-based brominated BH \ddot{E} s are calculated at B3LYP/TZ2P (Fig. 5). Interestingly, the p_y character of HOMO in heavier BH \ddot{E} s appears orthogonal to the σ (HOMO-1) orbital (Fig. 5, Table 9S).

The occupied σ orbital along with the unoccupied orthogonal p orbital in heavy divalent species of group 14 have attracted attention.^{43, 72} Quests continue to recognize their potential reaction molds and mechanistic studies in depth. The contribution of p in the hybrid orbital of divalent atom (E) in its \ddot{E} -B bond increases significantly while in contrast the s orbital in the hybrid orbital of \ddot{E} including the LP incorporates to a great extent (Table 6, 10S). This is an evidence for the stabilization of the singlet states with larger valance orbitals also known as the "inert s-pair effect", as mentioned previously.^{43, 72}

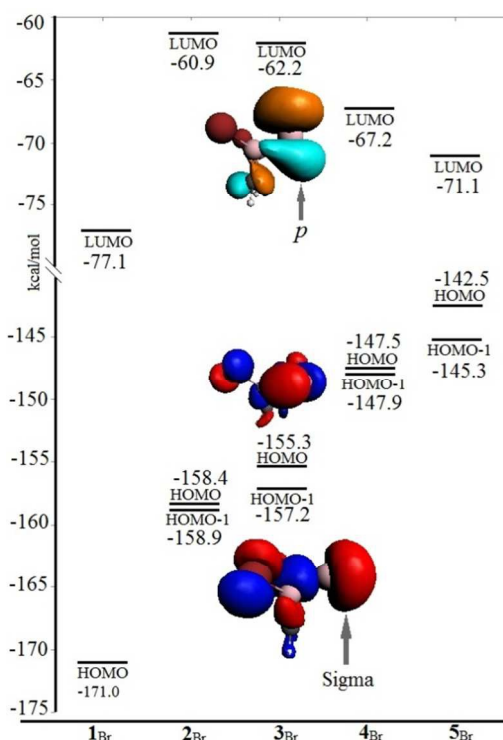


Fig. 5 Calculated frontier molecular orbital energies for carbene $\mathbf{1}_{\text{s-Br}}$, silylene $\mathbf{2}_{\text{s-Br}}$, germylene $\mathbf{3}_{\text{s-Br}}$, stannylene $\mathbf{4}_{\text{s-Br}}$, and plumbylene $\mathbf{5}_{\text{s-Br}}$ along with HOMO-1, HOMO and LUMO images for $\mathbf{3}_{\text{s-Br}}$.

Table 6 Average contributions (%) of s and p atomic orbitals in the hybrid orbitals of divalent atom (E).

	$\sigma_{\text{B-E}}$ bonds	LP orbital
$\mathbf{1}_X$	sp ^{0.99}	---
$\mathbf{2}_X$	sp ^{7.27}	sp ^{0.32}
$\mathbf{3}_X$	sp ^{10.42}	sp ^{0.21}
$\mathbf{4}_X$	sp ^{10.99}	sp ^{0.19}
$\mathbf{5}_X$	sp ^{12.16}	sp ^{0.16}

3.4.2 Linear relationships

Calculated energy differences between HOMO and LUMO of

singlet states, $\Delta E_{(\text{LUMO-HOMO})}$, for the halogenated BH \ddot{E} s appear to have linear relationships with the corresponding ΔE_{st} values. They show correlation coefficients (R^2) of 0.949, 0.914, 0.872 and 0.949 for $\mathbf{2}_X$, $\mathbf{3}_X$, $\mathbf{4}_X$, and $\mathbf{5}_X$ respectively (Fig. 6 and 3S).

As mentioned above, substitution of heavier group 14 atoms at the divalent centre increases the energy gap between HOMO-1 and HOMO with an increasing trend in going from carbon to lead. Such a substitution slightly decreases the energy of LUMO (known as p - π orbital), after sharing a sharp increase in carbenes (Fig. 5). Intriguingly, a reverse linear trend is observed for ΔE_{st} of BH \ddot{E} s vs. their corresponding band gap ($\Delta E_{(\text{LUMO-HOMO})}$) values (Fig. 6 and 3S). Evidently, the latter is concerned only with the singlet state while ΔE_{st} is associated with both singlet and triplet states. One may attribute this observation to the possibility of puckering in singlet species vs. its absence in the corresponding triplet states.

In accordance to discussion made on eqn 1, linear relationships are found between the B- \ddot{E} -B angles and their corresponding halogen atom radius, for the five-membered-rings: $\mathbf{2}_{\text{s-X}}$, $\mathbf{3}_{\text{s-X}}$, $\mathbf{4}_{\text{s-X}}$ and $\mathbf{5}_{\text{s-X}}$ with correlation factors of 0.844, 0.703, 0.970 and 0.990, respectively (Fig. 4S). This angle reduces with increasing the halogen atomic radius.⁷³

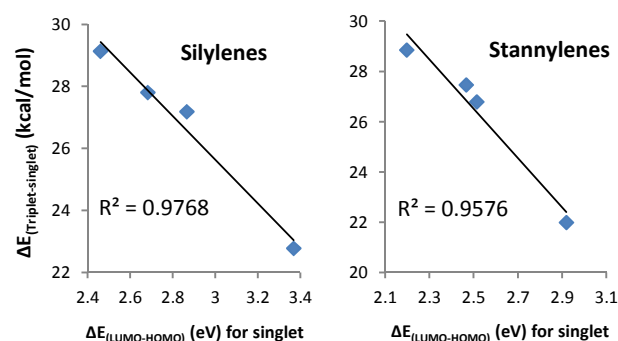


Fig. 6 Linear relationships between singlet LUMO-HOMO energy gaps $\Delta E_{(\text{LUMO-HOMO})}$, and their corresponding singlet-triplet energy separations (ΔE_{st}), for the two series of halogenated five-membered-rings: $\mathbf{3}_{\text{s-X}}$ and $\mathbf{5}_{\text{s-X}}$, with correlation factors: 0.914 and 0.949, respectively.

3.5 Electrophilicity and Nucleophilicity

Bis(boryl)-based heterocyclic carbenes ($\mathbf{1}_{\text{s-X}}$) show considerably stronger electrophilicity than their corresponding heavier group 14 homologues ($\mathbf{2}_{\text{s-X}}$ - $\mathbf{5}_{\text{s-X}}$) (Table 11S). In Arduengo's divalents (NH \ddot{E} s), this is reversed. Electrophilicity of $\mathbf{1}_{\text{s-X}}$ - $\mathbf{5}_{\text{s-X}}$ (X=F, Cl and Br, except for $\mathbf{1}_{\text{s-Br}}$) appear more than their corresponding halogenated NH \ddot{E} s. This may be due to the electron-deficiency of boron atoms. All iodinated BH \ddot{E} s show less electrophilic properties than their NH \ddot{E} homologues (Table 11S). This may partly be due to the higher significance of seesaw-type hyperconjugation interaction discussed above (Scheme 2a) where filling the vacant orbitals of boron atoms reduces the electrophilicity, specially for $\mathbf{5}_{\text{s-X}}$ (X=F, Cl, Br and I) species.

The nucleophilicity index for BH \ddot{E} s and equivalent NH \ddot{E} s increases from $\mathbf{1}_{\text{s-X}}$ through $\mathbf{5}_{\text{s-X}}$ (except for $\mathbf{5}_{\text{s-I}}$ in BH \ddot{E} s). The values of nucleophilicity for all NH \ddot{E} s (except $\mathbf{1}_{\text{s-F}}$) are greater than the homologues BH \ddot{E} s (Table 11S) which is expected.

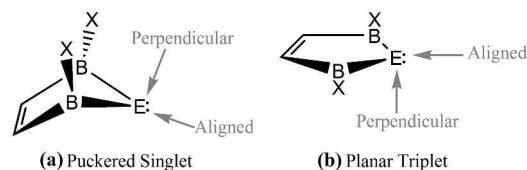
The singlet and triplet species have a σ^2 and $\sigma^1 p^1$ configuration

respectively which is obtained through a sequence of calculations documenting the interaction of the singlet and triplet species with Lewis acids and bases. The paths for approaching of the Lewis species to the singlet and triplet BHĒs are shown in scheme 3a and 3b, respectively.

For example, in the interaction of 2_{s-Cl} and 2_{t-Cl} with AlH_3 , approaching the Lewis acid from the aligned direction is more favourable and consumes less energy (Fig. 7). As Al gets closer to the Si atom, the energy increases, particularly for Si-Al distances lower than 250 pm (Fig. 7). Furthermore, while the singlet species (2_{s-Cl}) shows sensitivity toward the direction of AlH_3 approach, the triplet one (2_{t-Cl}) appears much less sensitive (Fig. 5S).

3.6 Isodesmic reactions

Isodesmic reactions suggest a high degree of correlation between ΔE_{st} and the relative energies of reaction with methane, coupling with hydroxymethylcarbene, and dimerization (Scheme 4). Firstly, reaction with methane (Scheme 4c) produces hydrogenated BHĒ and is defined as a measure for hydrogenation ($\Delta E_{hydrogenation}$).^{74, 75} Secondly, coupling with hydroxymethylcarbene (Scheme 4b) leads to the important Breslow-type intermediate.^{75, 76} Finally, dimerization (Scheme 4a) is an intrinsic reaction of divalents whose prevention increases the “Divalent Species Stabilization Energy; DSSE”.^{72, 77, 78}



Scheme 3

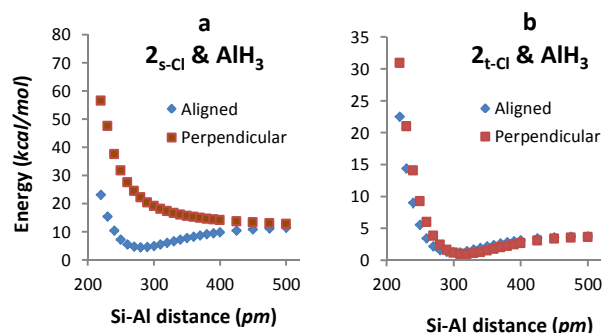
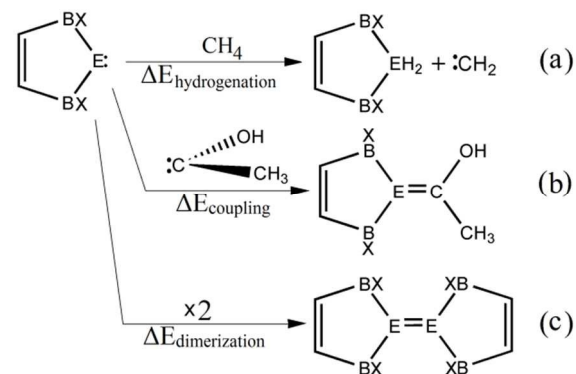


Fig. 7 Relative energies for the interactions of Lewis acid (AlH_3) with (a) 2_{s-Cl} and (b) 2_{t-Cl} .

Stannylenes (4_{s-X}) show the greatest values of $\Delta E_{hydrogenation}$ and hence are the most stable (Table 7). The general order for relative $\Delta E_{hydrogenation}$ is: $4_{s-X} > 3_{s-X} > 2_{s-X} > 5_{s-X} > 1_{s-X}$ ($X = F, Cl, Br, I$). This is except for 4_{s-I} which falls below the values for plumblylenes. Partially in each series, the BHĒ with $X = I$ shows the highest $\Delta E_{hydrogenation}$ (Scheme 4a). The order for the stability of the Breslow-type intermediates is: $5_{s-X} > 4_{s-X} > 3_{s-X} > 2_{s-X} > 1_{s-X}$ for $X = F, Cl, Br, I$ (Scheme 4b). The third reaction (with $\Delta E_{dimerization}$) shows an order of decreasing relative energy similar to the coupling reaction.



Scheme 4

As a result, the BHĒ gains more stability and shows less reactivity as the size of the divalent atom increases.

Table 7 Relative energies of hydrogenation ($\Delta E_{(a)}$), hydroxymethylcarbene coupling ($\Delta E_{(b)}$) and dimerization ($\Delta E_{(c)}$) in kcal/mol^a at B3LYP/TZ2P.

BHĒ	$\Delta E_{(a)}$	$\Delta E_{(b)}$	$\Delta E_{(c)}$	BHĒ	$\Delta E_{(a)}$	$\Delta E_{(b)}$	$\Delta E_{(c)}$
1_F	21	0	0	4_F	109	116	121
1_{Cl}	26	5	13	4_{Cl}	112	118	126
1_{Br}	26	5	15	4_{Br}	113	118	127
1_I	28	9	20	4_I	64	118	134
2_F	78	82	100	5_F	---	---	---
2_{Cl}	81	84	107	5_{Cl}	72	128	135
2_{Br}	81	84	108	5_{Br}	72	126	---
2_I	82	85	111	5_I	73	125	136
3_F	98	106	114	a The smaller values imply less stable BHĒs (easier reactivity).			
3_{Cl}	101	108	120				
3_{Br}	102	108	121				
3_I	103	109	123				

Correlation of the three reactions of our halogenated bis(boryl)-divalents (Fig. 8, 6S) appear consistent with the reactivity of divalent species previously concluded according to the effects of ΔE_{st} ,^{5, 43, 55, 72, 77} and divalent angle ($\angle BEB$).^{72, 77}

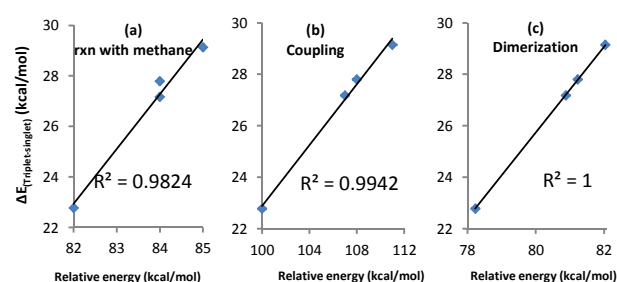


Fig. 8 Linear relationships between singlet-triplet energy separations (ΔE_{st}) of X_2 -BHĒs ($\ddot{E} = Si$; $X = F, Cl, Br, I$) and their relative energies of isodesmic reactions (a) with methane (b) coupling with hydroxymethylcarbene and (c) dimerization, as shown in scheme 4, respectively.

3.7 Complexation of BHĒ with group 11 metals

Possibility of interaction between BHĒs and group 11 chlorides ($CuCl, AgCl, AuCl$) are assessed (Table 12S). Each complexation energy is predicted through an isodesmic reaction $\Delta E_{complexation} = E_{complex} - (E_{BHE} + E_{MCl})$. The Au complexes appear the most exothermic, after which come the complexes of copper, followed by that of silver. On the other hand, the trend of ΔE for divalents complies with the following order:

$$1_X\text{-MCl} > 2_X\text{-MCl} > 3_X\text{-MCl}$$

Simultaneously, puckering angle (D1) of 1_X , 2_X , and 3_X (X=F, Cl) decreases significantly in the corresponding complex structures with the following trend:

$$\text{Cu} > \text{Ag} > \text{Au}$$

The decrease in WBI and donor-acceptor energies for $\ddot{\text{E}}-\text{M}$ proves this observation. WBI for B-B is considerably reduced, as well.

Calculations also reveal that the geometries around the metal atoms ($\angle\ddot{\text{E}}\text{-M-Cl}$), are not essentially linear, the most bent of which is for carbenes (1_X ; X=F, Cl) with an average angle of 170.90° . Silylenes, 2 , and germylenes, 3 , make more straight angles (an average of 178.58° and 177.8° for 2_X - and 3_X -MCl, respectively). In view of the metal atoms, the $\angle\ddot{\text{E}}\text{-M-Cl}$ in Cu complexes is smaller than the related angle in Ag and Au complexes.

The bond lengths $\ddot{\text{E}}\text{-B}$ in 1_X-MCl (X=F, Cl; M=Cu, Ag, and Au) are longer than in the free divalents (ligands). The trend is reversed in all complexes of 2_X and 3_X .

Every Au- $\ddot{\text{E}}$ bond is apparently shorter than the corresponding Ag- $\ddot{\text{E}}$ which is verified with WBI. The Cu- $\ddot{\text{E}}$ is shorter than both of them.

In view of the metal atom, π -back bonding energies ($\ddot{\text{E}}\leftarrow\text{MCl}$) obey the order of Au>Cu>Ag, which is in accordance with the above order of $\Delta E_{\text{complexation}}$ (Table 12S). Considering the divalent atom and consistent with the complexation energy order, the back donation descends from 1_X to 2_X and to 3_X . Therefore, 1_X-AuCl bears the most back-bonding energy and 3_X-AgCl is at the lowest end.

4. Conclusions

The challenging introduction of electron-withdrawing groups such as boryl substituents flanking the carbenic center ($\ddot{\text{E}}$) produces a good model of pull-pull carbene story profiting from the ability of boron to stabilize a LP in an adjacent position. Every bent singlet structure for all studied species is more stable than its corresponding planar triplet. Carbenes have the least stability among their corresponding heavier group 14 homologues. The stability of the singlets with a puckered geometry (D1 \cong 66 $^\circ$) is achieved *via* cross-ring hyperconjugative interactions, the most important of which we believe is a seesaw-type with a significant amount of bond index between the cross boron atoms (Scheme 2a, eqn 1) and a kind of $\pi\rightarrow p$ overlap between the divalent atom and the C=C bond (Scheme 2b, eqn 2), again with a notable amount of WBI (Table 5). These interactions make BH $\ddot{\text{E}}$ s ($\ddot{\text{E}}=\text{Si}$, Ge, Sn, Pb) considerably stable; the stability of which is demonstrated with singlet-triplet energy gaps (ΔE_{st}) and also proved by isodesmic reactions (Scheme 4). Moreover, eight species (2_{I} , 3_{Br} , 3_{I} , 4_{Br} , 4_{I} , 5_{Cl} , 5_{Br} , and 5_{I}) are found enjoying more stability than their corresponding NH $\ddot{\text{E}}$ homologues and three species (2_{Br} , 4_{Cl} , and 5_{F}) with comparable energies.

The σ^2 (sp^2) orbital in singlet species is HOMO in BHCs and HOMO-1 in heavier BH $\ddot{\text{E}}$ s with $\ddot{\text{E}}=\text{Si}$, Ge, Sn and Pb, while the electronic configuration for the triplets is $\sigma^1 p^1$.

There are linear relations between ΔE_{st} and $\Delta E_{(\text{LUMO-HOMO})}$ and also between ΔE_{st} and the atomic size of the divalent atom for each species.

The trend of the adduct formation energies of BH $\ddot{\text{E}}\text{-MCl}$ illustrate that for the ligands, the order for $\Delta E_{\text{complexation}}$ is carbene>silylene>germylene and for the metals Au>Cu>Ag. The most important change for the ligand geometries is the lengthening of the B- $\ddot{\text{E}}$ bond for $\ddot{\text{E}}=\text{C}$ and its shortening for $\ddot{\text{E}}=\text{Si}$ and Ge. The puckering of the BH $\ddot{\text{E}}$ s decreases in the structure of all surveyed complexes which is a consequence of decline in cross-hyperconjugations noticed in BH $\ddot{\text{E}}$ cycles. Obviously, such metal π -back-donation recompense the electron deficiency while increases the stability of the complex.

Acknowledgements

The authors are indebted to Prof. Hassan Sabzyan for his kind help and useful technical discussions.

Notes and references

^aDepartment of Chemistry, Payame Noor University (PNU), 19395-4697 Tehran, Iran. Fax: 00985138528520; Tel: 00989153114323; E-mail: a_akbari@pnu.ac.ir

^bDepartment of Chemistry, Tarbiat Modares University, Tehran, Iran.

Fax: +98 21 88006544; Tel: +98 09121000392; E-mail:

kassaem@modares.ac.ir (M.Z. Kassaee)

† Electronic Supplementary Information (ESI) available: [details of any supplementary information available should be included here]. See DOI: 10.1039/b000000x/

1. A. K. Guha, C. Das and A. K. Phukan, *Journal of Organometallic Chemistry*, 2011, 696, 586-593.
2. M. Z. Kassaee, M. R. Momeni, F. A. Shakib, Z. Najafi and H. Zandi, *Journal of Physical Organic Chemistry*, 2011, 24, 1022-1029.
3. W. Kirmse, *Angewandte Chemie International Edition*, 2010, 49, 8798-8801.
4. V. C. Rojisha, S. De and P. Parameswaran, *Inorganic Chemistry*, 2012, 51, 8265-8274.
5. C.-S. Wu and M.-D. Su, *Journal of Computational Chemistry*, 2011, 32, 1896-1906.
6. M. Z. Kassaee, H. Zandi, B. N. Haerizade and M. Ghambarian, *Computational and Theoretical Chemistry*, 2012, 1001, 39-43.
7. L. Broeckaert, P. Geerlings, A. R $\ddot{\text{A}}$ $\ddot{\text{A}}$ $\ddot{\text{A}}$ ka, R. Willem and F. D. Proft, *Organometallics*, 2012, 31, 1605-1617.
8. A. Chrostowska, V. Lemierre, A. Dargelos, P. Bayl $\ddot{\text{A}}$ $\ddot{\text{r}}$ e, W. J. Leigh, G. Rima, L. Weber and M. Schimmel, *Journal of Organometallic Chemistry*, 2009, 694, 43-51.
9. A. Bundhun, P. Ramasami, P. P. Gaspar and H. F. Schaefer, *Inorganic Chemistry*, 2012, 51, 851-863.
10. K. Izod, C. Wills, W. Clegg and R. W. Harrington, *Organometallics*, 2009, 28, 5661-5668.
11. D. Heitmann, T. Pape, A. Hepp, C. M $\ddot{\text{A}}$ $\ddot{\text{c}}$ k-Lichtenfeld, S. Grimme and F. E. Hahn, *Journal of the American Chemical Society*, 2011, 133, 11118-11120.
12. A. J. Arduengo, *Accounts of Chemical Research*, 1999, 32, 913-921.
13. A. J. Arduengo, R. L. Harlow and M. Kline, *Journal of the American Chemical Society*, 1991, 113, 361-363.
14. D. Bourissou, O. Guerret, F. o. P. Gabba $\ddot{\text{A}}$ $\ddot{\text{r}}$ and G. Bertrand, *Chemical Reviews*, 1999, 100, 39-92.
15. W. A. Herrmann and C. Köcher, *Angewandte Chemie International Edition in English*, 1997, 36, 2162-2187.

16. M. Denk, R. Lennon, R. Hayashi, R. West, A. V. Belyakov, H. P. Verne, A. Haaland, M. Wagner and N. Metzler, *Journal of the American Chemical Society*, 1994, 116, 2691-2692.
17. W. Kutzelnigg, *Angewandte Chemie International Edition in English*, 1984, 23, 272-295.
18. V. Y. Lee and A. Sekiguchi, in *Organometallic Compounds of Low-Coordinate Si, Ge, Sn and Pb*, John Wiley & Sons, Ltd, 2010, pp. 139-197.
19. P. Boudjouk, E. Black and R. Kumarathasan, *Organometallics*, 1991, 10, 2095-2096.
20. D. J. Lucas, L. A. Curtiss and J. A. Pople, *The Journal of Chemical Physics*, 1993, 99, 6697-6703.
21. M. R. Zachariah and W. Tsang, *The Journal of Physical Chemistry*, 1995, 99, 5308-5318.
22. A. Meller and C.-P. Gräbe, *Chemische Berichte*, 1985, 118, 2020-2029.
23. M. Veith and M. Grosser, *Z. Naturforsch.*, 1982, 37b, 1375-1381.
24. J. Barrau and G. Rima, *Coordination Chemistry Reviews*, 1998, 178-180, Part 1, 593-622.
25. N. Tokitoh and R. Okazaki, *Coordination Chemistry Reviews*, 2000, 210, 251-277.
26. A. E. Ayers, D. S. Marynick and H. V. R. Dias, *Inorganic Chemistry*, 2000, 39, 4147-4151.
27. J. R. Babcock, C. Incarvito, A. L. Rheingold, J. C. Fettinger and L. R. Sita, *Organometallics*, 1999, 18, 5729-5732.
28. H. V. R. Dias and W. Jin, *Journal of the American Chemical Society*, 1996, 118, 9123-9126.
29. T. Gans-Eichler, D. Gudat and M. Nieger, *Angewandte Chemie International Edition*, 2002, 41, 1888-1891.
30. P. J. Davidson, D. H. Harris and M. F. Lappert, *Journal of the American Chemical Society*, *Dalton Transactions*, 1976, 2268-2274.
31. P. J. Davidson and M. F. Lappert, *Journal of the Chemical Society, Chemical Communications*, 1973, 317a-317a.
32. M. Weidenbruch, *Journal of Organometallic Chemistry*, 2002, 646, 39-52.
33. J. P. H. Charmant, M. F. Haddow, F. E. Hahn, D. Heitmann, R. Frohlich, S. M. Mansell, C. A. Russell and D. F. Wass, *Dalton Transactions*, 2008, 6055-6059.
34. B. Gehrhus, P. B. Hitchcock and M. F. Lappert, *Journal of the American Chemical Society*, *Dalton Transactions*, 2000, 3094-3099.
35. Y. Ishida, B. Donnadiou and G. Bertrand, *Proceedings of the National Academy of Sciences*, 2006, 103, 13585-13588.
36. M. M. Brahmī, J. Monot, M. Desage-El Murr, D. P. Curran, L. Fensterbank, E. Lacôte and M. Malacria, *The Journal of Organic Chemistry*, 2010, 75, 6983-6985.
37. J. Monot, A. Solovyev, H. Bonin-Dubarle, É. Derat, D. P. Curran, M. Robert, L. Fensterbank, M. Malacria and E. Lacôte, *Angewandte Chemie International Edition*, 2010, 49, 9166-9169.
38. A. Solovyev, Q. Chu, S. J. Geib, L. Fensterbank, M. Malacria, E. Lacôte and D. P. Curran, *Journal of the American Chemical Society*, 2010, 132, 15072-15080.
39. S.-H. Ueng, A. Solovyev, X. Yuan, S. J. Geib, L. Fensterbank, E. Lacôte, M. Malacria, M. Newcomb, J. C. Walton and D. P. Curran, *Journal of the American Chemical Society*, 2009, 131, 11256-11262.
40. M. Yamashita, *Angewandte Chemie International Edition*, 2010, 49, 2474-2475.
41. C.-H. Chen and M.-D. Su, *Inorganic Chemistry*, 2006, 45, 8217-8226.
42. F. Lavigne, E. Maerten, G. Alcaraz, N. Saffon-Merceron, C. Acosta-Silva, V. Branchadell and A. Baceiredo, *Journal of the American Chemical Society*, 2010, 132, 8864-8865.
43. C.-S. Wu and M.-D. Su, *Dalton Transactions*, 2012, 41, 3253-3265.
44. H. Meyer, G. Baum, W. Massa, S. Berger and A. Berndt, *Angewandte Chemie International Edition in English*, 1987, 26, 546-548.
45. H. Meyer, G. Baum, W. Massa and A. Berndt, *Angewandte Chemie International Edition in English*, 1987, 26, 798-799.
46. A. V. Protchenko, K. H. Birjkumar, D. Dange, A. D. Schwarz, D. Vidovic, C. Jones, N. Kaltsoyannis, P. Mountford and S. Aldridge, *Journal of the American Chemical Society*, 2012, 134, 6500-6503.
47. M. Z. Kassaee, J. Azarnia and S. Arshadi, *Journal of Molecular Structure: THEOCHEM*, 2004, 686, 115-122.
48. M. Z. Kassaee, B. N. Haerizade and S. Arshadi, *Journal of Molecular Structure: THEOCHEM*, 2003, 639, 187-193.
49. M. Z. Kassaee, Z. S. Hossaini, B. N. Haerizade and S. Z. Sayyed-Alangi, *Journal of Molecular Structure: THEOCHEM*, 2004, 681, 129-135.
50. M. Z. Kassaee, M. R. Nimlos, K. E. Downie and E. E. Waali, *Tetrahedron*, 1985, 41, 1579-1586.
51. M. Z. Kassaee, S. Z. Sayyed-Alangi and Z. Hossaini, *Journal of Molecular Structure: THEOCHEM*, 2004, 676, 7-14.
52. H. Dürr and F. Wernsdorff, *Angewandte Chemie International Edition in English*, 1974, 13, 483-484.
53. C. Lee, W. Yang and R. G. Parr, *Physical Review B*, 1988, 37, 785-789.
54. M. J. Frisch, J. A. Pople and J. S. Binkley, *The Journal of Chemical Physics*, 1984, 80, 3265-3269.
55. M.J. Frisch, G.W. Trucks, H.B. Schlegel, G.E. Scuseria, M.A. Robb, J.R. Cheeseman, V.G. Znkzowski, G.A. Montgomery, R.E. Startmann, J.C. Burant, S. Dapprich, J.M. Millam, A.D. Daniels, K.N. Kudin, M.C. Strain, O. Farkas, J. Tomasi, V. Barone, M. Cossi, R. Cammi, B. Mennucci, C. Pampelli, G. Adamo, S. Clifford, J. Ochterski, G.A. Petersson, P.Y. Ayala, Q. Cui, K. Morokoma, D.K. Malick, A.D. Rubuck, K. Raghavachari, J.B. Foresman, J. Cioslowski, J.V. Ortiz, B.B. Stefanov, G. Liu, A. Liashenko, P. Piskorz, I. Komaromi, R. Comperts, R.L. Martin, P.J. Fox, T. Keith, M.A. Al-laham, C.Y. Peng, A.N. Akkara, C.G. Gonzales, M.C. Combe, P.M.W. Gill, B. Johnson, W. Chem, M.W. Wong, J.L. Andres, C. Gonzales, M. Head-Gordon, E.S. Replogle and J.A. Pople, *GAUSSIAN 98*, 1998, Revision A. 6, Gaussian Inc., Pittsburgh, PA.
56. *ADF2008.01, SCM, Theoretical Chemistry, Vrije University, Amsterdam, the Netherlands. Available from: <http://www.scm.com>.*
57. C. Fonseca Guerra, J. G. Snijders, G. te Velde and E. J. Baerends, *Theoretical Chemistry Accounts*, 1998, 99, 391-403.

58. G. te Velde, F. M. Bickelhaupt, E. J. Baerends, C. Fonseca Guerra, S. J. A. van Gisbergen, J. G. Snijders and T. Ziegler, *Journal of Computational Chemistry*, 2001, 22, 931-967.
59. M. P. McGrath and L. Radom, *The Journal of Chemical Physics*, 1991, 94, 511-516.
60. L. A. Curtiss, M. P. McGrath, J. P. Blaudeau, N. E. Davis, R. C. Binning and L. Radom, *The Journal of Chemical Physics*, 1995, 103, 6104-6113.
61. H. B. Schlegel and M. J. Frisch, *International Journal of Quantum Chemistry*, 1995, 54, 83-87.
62. E. v. Lenthe, E. J. Baerends and J. G. Snijders, *The Journal of Chemical Physics*, 1993, 99, 4597-4610.
63. E. van Lenthe, E. J. Baerends and J. G. Snijders, *The Journal of Chemical Physics*, 1994, 101, 9783-9792.
64. E. van Lenthe, A. Ehlers and E.-J. Baerends, *The Journal of Chemical Physics*, 1999, 110, 8943-8953.
65. E. van Lenthe, J. G. Snijders and E. J. Baerends, *The Journal of Chemical Physics*, 1996, 105, 6505-6516.
66. E. van Lenthe, R. van Leeuwen, E. J. Baerends and J. G. Snijders, *International Journal of Quantum Chemistry*, 1996, 57, 281-293.
67. Y. Zhao and D. G. Truhlar, *Journal of Chemical Theory and Computation*, 2008, 4, 1849-1868.
68. L. Goerigk and S. Grimme, *Journal of Chemical Theory and Computation*, 2011, 7, 291-309.
69. W. C. McKee, J. I. Wu, M. Hofmann, A. Berndt and P. v. R. Schleyer, *Organic Letters*, 2012, 14, 5712-5715.
70. F. Weinhold and C. R. Landis, *Valency and Bonding: A Natural Bond Orbital Donor-Acceptor Perspective*, Cambridge University Press, 2005.
71. Y. Xiong, S. Yao, S. Inoue, J. D. Epping and M. Driess, *Angewandte Chemie International Edition*, 2013, 52, 7147-7150.
72. J.-Y. Chen and M.-D. Su, *Dalton Transactions*, 2011, 40, 7898-7907.
73. B. D. Rekker, T. M. Brown, J. C. Fettinger, F. Lips, H. M. Tuononen, R. H. Herber and P. P. Power, *Journal of the American Chemical Society*, 2013, 135, 10134-10148.
74. A. A. Tukov, A. T. Normand and M. S. Nechaev, *Dalton Transactions*, 2009, DOI: 10.1039/B906969K, 7015-7028.
75. O. Hollóczki, Z. Kelemen and L. Nyulászi, *The Journal of Organic Chemistry*, 2012, 77, 6014-6022.
76. M. Veith and M. Grosser, *Z. Naturforsch*, 1982, 37b, 1375-1381.
77. R.-H. Wang and M.-D. Su, *The Journal of Physical Chemistry A*, 2008, 112, 7689-7698.
78. L. Nyulászi, T. Veszpremi and A. Forro, *Physical Chemistry Chemical Physics*, 2000, 2, 3127-3129.